www.elsevier.nl/locate/jorganchem

Journal of Organometallic Chemistry 587 (1999) 244–251

Selective dynamics of [Rh(1,5-COD)(bidentate)]BF_4 complexes via NMR exchange spectroscopy

Massimiliano Valentini, Kumaravel Selvakumar, Michael Wörle, Paul S. Pregosin *

Laboratory of Inorganic Chemistry, ETH Zentrum, CH-8092 Zurich, Switzerland

Received 15 March 1999

Abstract

NMR exchange measurements on [Rh(1,5-COD)(bidentate)]BF_4 complexes (bidentate = chiral bis-phosphine, a P,N-phosphino-oxazoline, a P,S-phosphito-thioether and a bis-pyrazolylborate) show selective 1,5-COD dynamics which can be superficially attributed to olefin rotation. It is suggested that the mechanism actually involves: (i) M–L^1 bond breaking (L^1 = N or S-donor); (ii) isomerization of the T-shaped species; (iii) rotation around the remaining M–L^2 bond and (iv) recomplexation. The solid state structures of the two compounds [M(1,5-COD)(**10**)]BF_4, M = Rh, Ir and **10** = (*S*,*R*)-2-[4-(isopropyl)oxazol-2-yl]-2′-diphenylphosphino-1,1′-binaphthyl, were determined by X-ray diffraction methods. © 1999 Elsevier Science S.A. All rights reserved.

Keywords: [Rh(1,5-COD)(bidentate)]$^+$; 2 D-Exchange NMR; X-ray diffraction

1. Introduction

Four-coordinate cationic olefin (and especially 1,5-COD) tertiary-phosphine complexes of Rh(I) are commonly used precursors in homogeneous catalytic hydrogenation [1–6]. The ^{13}C-NMR characteristics of these species have been routinely registered over the years as models for metal–olefin bonding [7], and there are numerous X-ray diffraction studies on these compounds [6,8–15]. However, little attention has been given to the solution dynamics of this class of cationic olefin compounds. Chaloner and co-workers [13] have reported stereochemical non-rigidity in the ferrocene cation **1**; however they attribute this to changes in the phosphine chelate ring conformation.

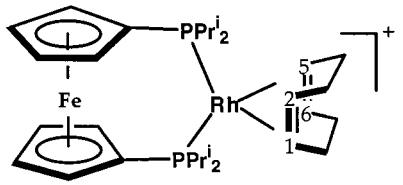

1

The P,N-complexes **2** [14] and **3** [15] are also dynamic in solution and these molecules are thought to show dynamic behaviour that arises via nitrogen dissociation.

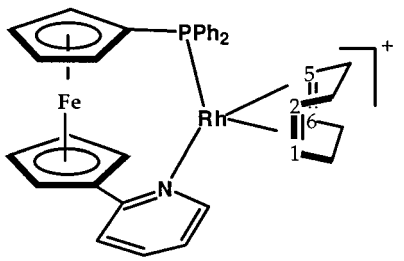

2

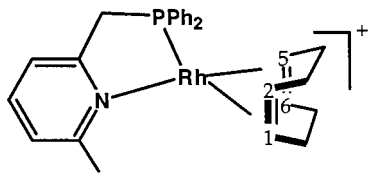

3

We have recently reported the synthesis of the Rh(I) complexes **4** [16] (a dinuclear species which contains two PO, PN bidentate ligands) and the *exo*-norborneol thioether complex **5** [17].

* Corresponding author. Tel.: +41-1-632291; fax: +41-1-6321090.
E-mail address: pregosin@inorg.chem.ethz.ch (P.S. Pregosin)

PII: S0022-328X(99)00329-0

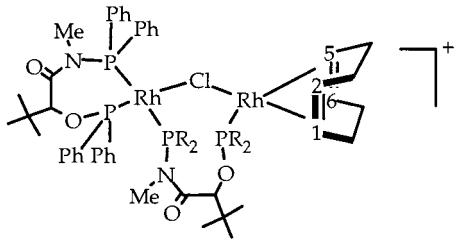

4, R = Ph

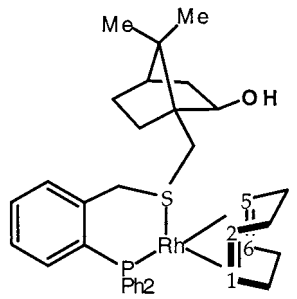

5

Both of these compounds show slow and selective exchange of the olefinic protons 1 and 2, with 5 and 6, respectively, i.e. apparent rotation of the 1,5-COD chelate. This type of olefin exchange selectivity has also been observed [18] for the olefinic protons of the chiral cation [Rh(norbornadiene)(**6**)]$^+$.

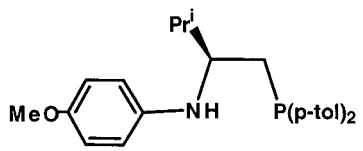

6

It seemed of interest to determine whether similar molecular dynamics are observable in a wider variety of chelating cationic 1,5-COD complexes. To this end we have used the chelating ligands **7**–**11**, to prepare the compounds [Rh(1,5-COD)(**7**–**11**)]BF_4, **12**–**16**, as shown in Scheme 1, and studied their solution characteristics using NMR exchange spectroscopy.

2. Results

2.1. X-ray structures of *15a,b*

The preparation of the Rh(I) (and one Ir(I)) 1,5-COD complexes followed standard literature procedures. As auxiliary **10** is relatively new we have grown crystals of the Rh(I) and Ir(I) P,N-complexes, **15a,b**, and determined their structures via X-ray diffraction. Figs. 1 and 2 show views for these Rh(I) and Ir(I) cations and Table 1 gives selected bond angles and bond lengths for these compounds. Fig. 1 provides a view from above the P–Rh–N coordination plane of the Rh(I) complex, whereas Fig. 2 shows the Ir(I) complex from behind the 1,5-COD.

The two structures are remarkably similar. The metal atom is found in a distorted square-planar environment and the 1,5-COD ligand is significantly rotated with respect to the N(1)–M–P(3) plane, e.g. the angles P(3)–M–C(43), 148.3(2)°, 146.4(2)° and P(3)–M–C(44), 175.4(2)° and 176.6(2)° are quite different (the double bond C(39)–C(40) is *trans* to N and C(43)–C(44) *trans* to P). The coordination bond lengths and remaining bond angles are in keeping with the literature [6,8–18], although it is noteworthy that **15a** and **15b** both show N(1)–M–P(3) angles several degrees below 90°. Binap complexes have P–M–P angles $>90°$ [10,19,20]. The complexed double bonds show C–C bond distances which are consistent with the idea that (i) there is π-back bonding from the metal to the olefin and (ii) Ir(I) is somewhat electron richer than Rh(I). As in the two previous structures of this ligand [21], the oxazoline ring is ca. perpendicular to the N(1)–M–P(3) plane and this is best seen in Fig. 2. The P–Ir–N plane is shown as almost horizontal and the O(1)–C–N(1) plane of the oxazoline can be clearly seen to be forced away from the former plane.

2.2. NMR spectroscopy for the complexes

Table 2 gives a selection of ^{1}H-, ^{13}C-, and ^{31}P-NMR data for the 1,5-COD complexes, and includes

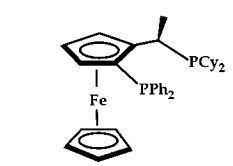

7

[Rh(1,5-COD)(**7**)]$^+$ = **12**

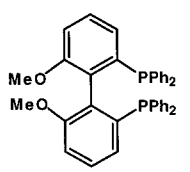

8

[Rh(1,5-COD)(**8**)]$^+$ = **13**

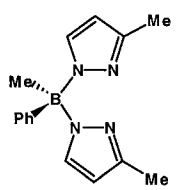

9

[Rh(1,5-COD)(**9**)]$^+$ = **14**

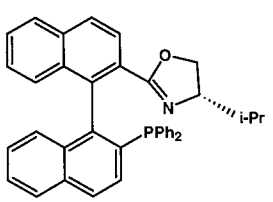

10

[Rh(1,5-COD)(**10**)]$^+$ = **15a**

[Ir(1,5-COD)(**10**)]$^+$ = **15b**

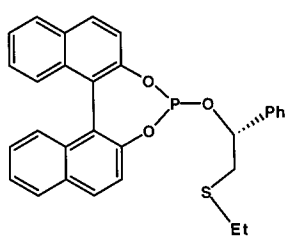

11

[Rh(1,5-COD)(**11**)]$^+$ = **16**

Scheme 1. Ligands and their Rh(1,5-COD) complexes as BF_4 salts.

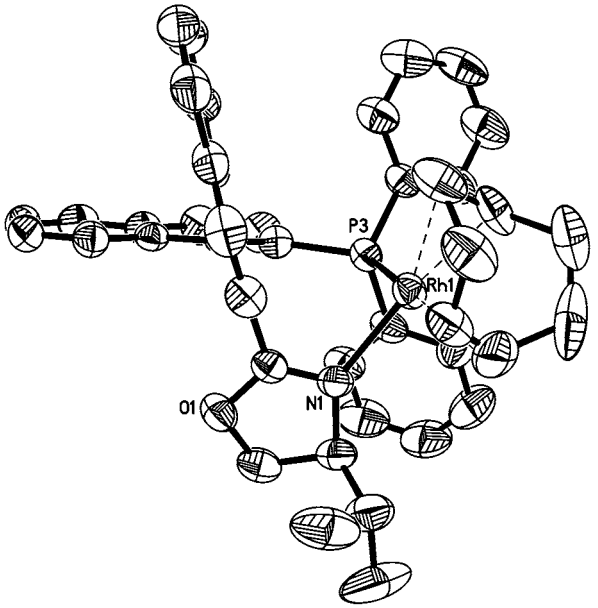

Fig. 1. View of the cation of the rhodium P,N 1,5-COD complex **15a**.

$^1J(^{103}Rh,^{13}C$, olefin) values which fall in the range 5–13 Hz. The usual NOESY, C–H and P–H methods were used to make the necessary assignments [22,23]. The two bis-phosphine cations, [Rh(1,5-COD)(**7**)]$^+$ (**12**) and [Rh(1,5-COD)(**8**)]$^+$ (**13**), and the pyrazolyl borate

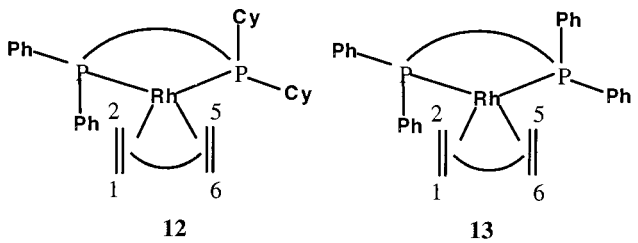

12 **13**

fragments of **12** and **13** showing

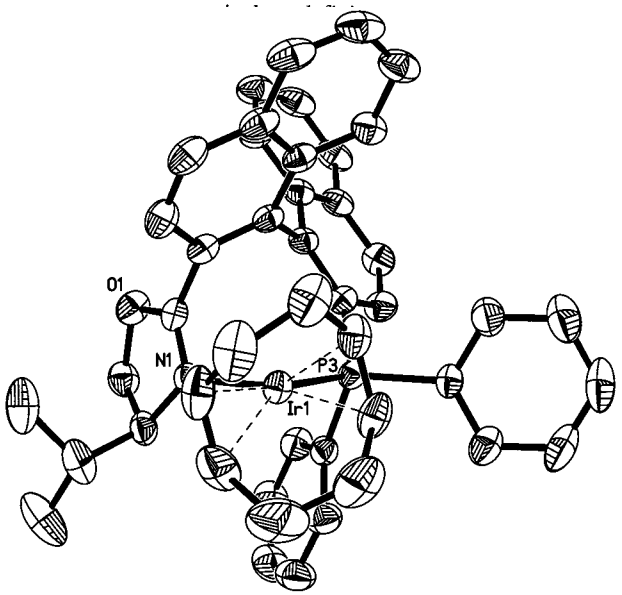

Fig. 2. View of the cation of the iridium P,N 1,5-COD complex **15b**.

Table 1
Selected bond lengths (Å) and bond angles (°) for the cations **15a** and **15b** [a]

	15a (Rh)	**15b** (Ir)
M–P(3)	2.3103(12)	2.3029(9)
M–N(1)	2.170(4)	2.151(3)
M–C(39)	2.106(6)	2.109(4)
M–C(40)	2.146(5)	2.142(4)
M–C(43)	2.182(6)	2.156(4)
M–C(44)	2.229(5)	2.206(4)
C(1)–N(1)	1.270(6)	1.274(5)
C(1)–O(1)	1.340(6)	1.339(5)
C(39)–C(40)	1.363(9)	1.399(7)
C(43)–C(44)	1.376(10)	1.383(8)
N(1)–M–P3	86.53(11)	86.62(9)
P(3)–M–C(39)	97.51(18)	97.68(13)
P(3)–M–C(40)	91.89(16)	92.21(12)
P(3)–M–C(43)	148.3(2)	146.4(2)
P(3)–M–C(44)	175.4(2)	176.6(2)
N(1)–M–C(39)	152.0(2)	150.7(2)
N(1)–M–C(40)	170.6(2)	171.0(2)
N(1)–M–C(43)	94.3(2)	95.0(2)
N(1)–M–C(44)	93.5(2)	92.6(2)

[a] C(39)–C(40) *trans* to N; C(43)–C(44) *trans* to P.

analog, **14** were prepared in order to have complexes with the same two donor atoms.

For the ferrocene phosphine complex **12**, NOE spectroscopy, using the *o*-phenyl PPh_2 and the PCy_2 aliphatic protons, allows the four non-equivalent 1,5-COD olefinic protons and carbons 1,2 and 5,6 to be assigned. Exchange spectroscopy [24] on this bis-phosphine compound reveals no olefin exchange at ambient temperature. Complex **12** contains relatively good P-donors, as evidenced by the observed relatively high-frequency ^{13}C chemical shifts of the olefin carbons (i.e. the chelating phosphine has the expected *trans* influence). Assuming 'olefin rotation' to be the mechanism for the dynamics noted above, it is not obvious why it should be suppressed in **12**. In the MeO–Biphep complex **13**, the two non-equivalent 1,5-COD olefinic resonances arise due to the axial and equatorial orientation of the P-phenyl substituents. Complex **13** is not expected to show exchange due to 'rotation' but is a useful compound in that its 2 D spectrum confirms that no other exchange is observed.

On the other hand, the pyrazolyl-borate, **14**, P,N, **15** and P,S-chelate complexes, **16**, all show the selective olefin exchange noted above for **4**–**6** (protons 1 and 2, with 5 and 6, respectively), although routine $^1J(^{103}Rh,^{13}C$, olefin) values are observed. Fig. 3 shows sections of the ^1H-NMR exchange spectra for **15a** (top) and **16** (bottom). In both of these, there are two relatively high-frequency absorptions (olefin protons *trans* to P), which are in selective slow exchange with

two lower frequency signals. The bis pyrazolyl-borate derivative **14** (Fig. 4), shows two COD olefin environments, 1 and 6 on one side of the N–Rh–N plane and 2 and 5 on the other (see **17**). Its 2 D exchange spectrum is especially clear in that the pairwise exchange of both olefinic and aliphatic resonances is clearly observed. These dynamics exchange the two olefin (or methylene groups) on the side of the B–Ph with the two on the side of the B–Me.

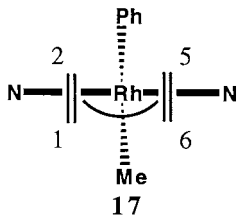

17

View from behind the COD showing the relative positions of the olefinic protons in **14**. The B-atom is obscured by the Rh-atom

3. Discussion

Since very different complexes such as **4** and **5** (amongst others) as well as **14**–**16** reveal related 1,5-COD dynamics, the chemistry involved has some generality. We attribute these results to a mechanism whose first step involves Rh–L^1 bond breaking (L^1 = N or S donor) to form a three-coordinate species (see Scheme 2). Rearrangement of the T-shape three-coordinate formed is followed by rotation around the remaining P– or N–Rh bond. Recombination of the N (or S) L^1 donor completes the mechanism. This sequence (and especially step 3, the rotation of a large structural fragment) is expected to be relatively slow. We have no direct evidence for M–L^1 bond breaking; however, a mechanism related to ours has been postulated in Pd–allyl chemistry (i.e. allyl rotation is not proposed) [22,25].

With the chelating bis-phosphines, **12** and **13**, containing two relatively strong donors, Rh–P dissociation is less likely, and thus the dynamics are not observed. 1,5-COD olefin rotation, which would involve breaking two bonds simultaneously, is excluded based on the observations of the bis-phosphine complexes. It is always possible that a five-coordinate species is responsible for the observed dynamics. The fifth ligand might come from the BF_4 anion; however, traces of water must also be considered. To this end we have added more than a 10-fold excess of water to the previously recorded solution of **14** and remeasured the exchange spectrum. The result is unchanged within the experimental error, i.e. a significant increase in the concentration of water does not accelerate (or hinder) the exchange dynamics. As one expects the water to solvolyse the BF_4 anion, this result also represents indirect evidence that the BF_4^- is not involved.

For several of the complexes inverse spectroscopy via the olefinic proton resonances was employed to obtain the rhodium-103 chemical shifts and, for **16**, this result is shown in Fig. 5. It is interesting to note that there are very strong cross-peaks arising from all four SCH_2 resonances (in addition to cross-peaks from the COD protons). Our experience [17] suggests that the three-bond Rh–S–C–H interactions can be >2 Hz, so that, generally speaking, ^{103}Rh-chemical shifts in thioether complexes might well be easily accessible. Since the dynamics noted above are relatively slow (estimated to be <0.5/s), and the spin-spin coupling to ^{103}Rh in **16** relatively large, Rh–S bond breaking (the first step in

Table 2
Selected olefin NMR data for the 1,5-COD complexes

δ	**12** [a]	**13** [b]	**14** [c]	**15a** [d]	**15b** [e]	**16** [f]
(H-1)	5.56	4.81	4.47	5.12	5.22	5.74
(H-2)	5.36	4.50	4.47	5.05	4.42	5.95
(H-5)	4.32	4.81	3.61	3.13	2.97	5.10
(H-6)	3.32	4.50	3.61	3.30	3.06	3.67
(C-1)	97.6	98.0	78.0	99.1 (q)	89.7	113.6
(C-2)	93.3	102.8	78.0	97.6 (q)	82.4	116.5
(C-5)	95.8	98.0	80.2	82.5 (d)	72.8	92.1
(C-6)	101.2	102.8	80.2	77.4 (d)	62.4	86.6
(P)	21.4 53.5 [a]	25.7	–	21.7 (d)	18.5 (s)	137.6 (d)

[a] ^1J(Rh,P), PCy_2 = 150 Hz, ^2J(P,P) = 32 Hz, PPh_2 resonance is broad.
[b] ^1J(Rh,P) = 146 Hz, ^1J(Rh,C, olefin) = 7.8 Hz.
[c] ^1J(Rh,C, olefin) = ca. 13 Hz.
[d] ^1J(Rh,C, olefin) = 8.1, 8.7, 12.4 and 12.2 Hz for the 99.1, 97.6, 82.5 and 77.4 ppm signals, respectively.
[e] ^2J(P,C) = 10.7 and 15.0 Hz, respectively, for the 89.7 and 82.4 ppm signals.
[f] ^1J(Rh,C, olefin) = 5.0, 5.7, 10.1 and 9.2 Hz for the 116.5, 113.6, 92.1 and 86.6 ppm signals, respectively.

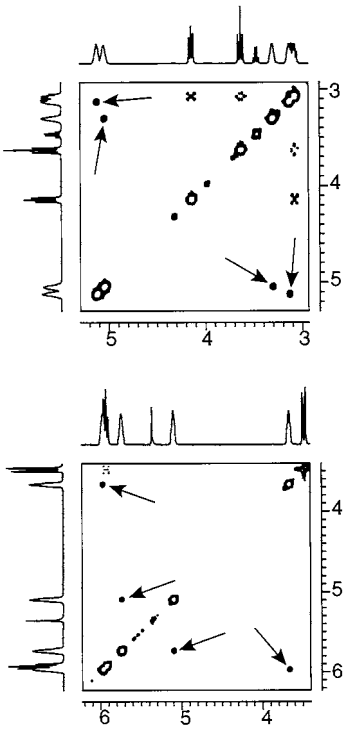

Fig. 3. Sections of the exchange spectrum for the P,N compound **15a** (top) and the P,S complex **16** (bottom). The exchange cross-peaks are indicated by arrows. In each case there are four non-equivalent 1,5-COD olefinic protons (two at high frequency, *trans* to P and two at low frequency, *trans* to either N or S), which are in selective exchange (400 MHz, CD_2Cl_2).

the suggested mechanism) is not in contradiction to the observed cross-peaks due to the three-bond coupling.

In conclusion, several, but not all, of the Rh(1,5-COD)(L^1,L^2 chelate)$^+$ cations are dynamic, with the NMR observations consistent with apparent rotation of the 1,5-COD. However, we suggest that a different mechanism involving Rh–L^1 bond breaking is operative, so that, taken together with molecules such as **2**–**5** a general mechanistic picture is slowly emerging.

4. Experimental

4.1. General

All manipulations were carried out under an argon atmosphere. Diethyl ether was distilled from sodium-benzophenone ketyl, CH_2Cl_2 from CaH_2, and hexane from sodium. (*S*,*R*)-2-[4-(Isopropyl)oxazol-2-yl]-2′-diphenylphosphino-1,1′-binapthyl (**10**) was prepared as reported earlier [21]. Ligand **11** has been prepared in our laboratory and its synthesis and further chemistry will be reported separately. $[Rh(COD)_2]BF_4$ and $[Ir(COD)_2]BF_4$ were prepared [26] from $[Rh(COD)Cl]_2$ and $[Ir(COD)Cl]_2$, respectively.

Routine ^{1}H-, ^{13}C- and ^{31}P-NMR spectra were

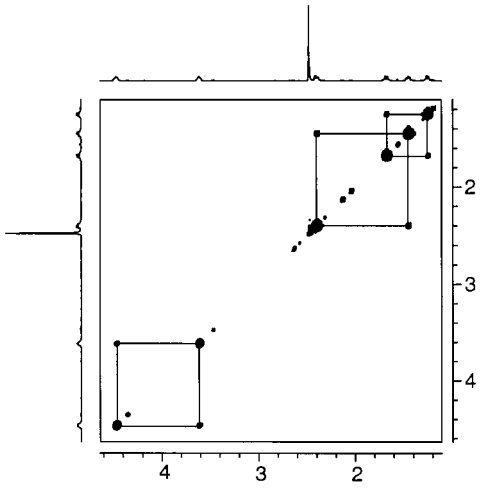

Fig. 4. Section of the exchange spectrum for the N,N compound **14**. The exchange cross-peaks are indicated by rectangles. In this complex the olefinic and aliphatic protons of the 1,5-COD are well resolved. The four different aliphatic CH_2 signals show pairwise exchange (400 MHz, CD_2Cl_2).

recorded with Bruker DPX-250, 300 and 400 MHz spectrometers. Chemical shifts are given in ppm and coupling constants (*J*) in Hz. The phase-sensitive two-dimensional ^{1}H-NOESY and ^{31}P–^{1}H (and ^{13}C–^{1}H) correlation experiments were carried out at 400 MHz [22,23].

4.2. X-ray crystallographic studies

Table 3 shows crystal data and structure refinement parameters for **15a**(Rh) and **15b**(Ir). Intensity data for both complexes were collected on a Siemens SMART PLATFORM equipped with a CCD detector. An empirical absorption correction was performed with SADABS [27]. The Bruker program package SHELXTL Version 5 [28] was used for the structure solution (direct meth-

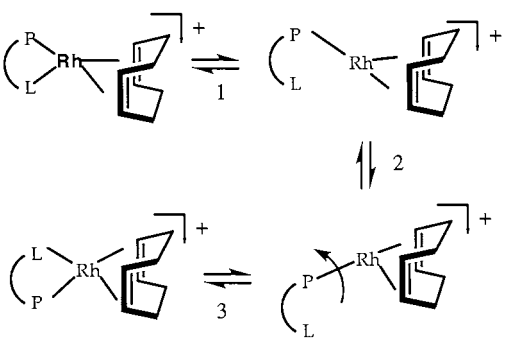

Mechanism of the dynamics for **15a** and **16**.

Step 4, recomplexation of L (not shown), follows step 3, rotation.

Scheme 2.

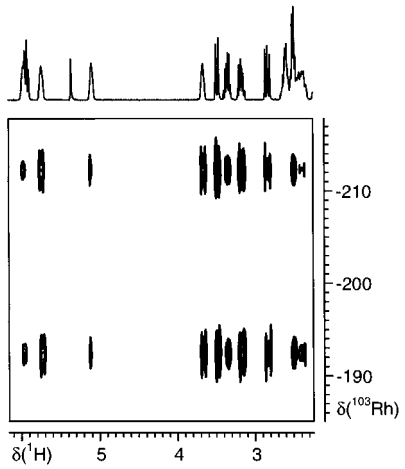

Fig. 5. Inverse ^{103}Rh spectrum for **16** showing the numerous contacts due to $J(^{103}Rh,^{1}H)$ coupling. The separation of the two horizontal cross-peaks represents the one-bond rhodium–phosphorus coupling constant. There are four strong cross-peaks in the region ca. 2.83–3.48 ppm, stemming form the four non-equivalent SCH_2 protons.

ods), structure refinement (full-matrix least-squares on F^2) and molecular graphics. In **15a** the BF_4 molecule is disordered. Further, a disordered solvent (dichloromethane) molecule was found and described with 6.3 carbon equivalents per formula unit. Disorder of a part of the solvent molecules was also found in **15b** and described with 1.5 carbon equivalents. All non-hydrogen atoms except the atoms belonging to the disordered atoms were refined with anisotropic thermal displacement parameters. All hydrogen atoms were placed at calculated positions, and refined (riding model) with different isotropic thermal displacement parameters for each group.

4.2.1. Complex ***15a***

A solution of $[Rh(COD)_2]BF_4$ (20 mg, 0.05 mmol) and ligand **10** (28 mg, 0.05 mmol) in CH_2Cl_2 (2 ml) was stirred at room temperature (r.t.) for 2 h. The solvent was evaporated i.v. and the residue was washed with hexane. The complex (**15a**) obtained was recrystallised from CH_2Cl_2–ether. Yield: 38 mg, 91%. MS (FAB): 760 (M^+–BF_4^-) (100), 652 [M^+–(COD + BF_4^-)] (40). A single crystal suitable for X-ray diffraction was obtained by slow diffusion of ether into the CH_2Cl_2 solution. Anal. Calc. for $C_{46}H_{44}NOBF_4PRh$ (847.54): C, 65.19; H, 5.23; N. 1.65. Found: C, 65.12; H, 5.32; N, 1.55. ^{1}H-NMR (CD_2Cl_2, 298 K, 400 MHz): 5.12 (br, *H*-1), 5.05 (br, *H*-2), 4.14 (dd, $^2J_{HH} = 11.1$, $^3J_{HH} = 7.9$, *cis* C*H*O), 3.63 (t, $^2J_{HH} = 11.0$, $^3J_{HH} = 9.3$, *trans* C*H*O), 3.30 (br, *H*-6), 3.13 (br, *H*-5), 3.08 (m, C*H*N), 2.38 (m, *H*-8), 2.22 (m, *H*-3), 2.06 (m, *H*-3′ and *H*-8′), 1.94 (m,

Table 3
Crystal data and structure refinement for **15a**(Rh) and **15b**(Ir)

Identification code	**15a**(Rh)	**15b**(Ir)
Empirical formula	$C_{46}H_{44}BF_4NOPRh{\cdot}CH_2Cl_2$	$C_{46}H_{44}BF_4NOPIr{\cdot}0.5C_4H_{10}O{\cdot}1.5C$
Formula weight	932.44	991.88
Temperature (K)	293(2)	233(2)
Wavelength (Å)	0.71073	0.71073
Crystal system	Orthorhombic	Orthorhombic
Space group	$P2_12_12_1$	$P2_12_12_1$
Unit cell dimensions		
a (Å)	10.8193(16)	10.7634(16)
b (Å)	17.826(3)	17.422(3)
c (Å)	23.002(4)	23.516(4)
V (Å^3)	4436.3(12)	4409.8(11)
Z	4	4
$D_{calc.}$ (Mg m^{-3})	1.396	1.494
Absorption coefficient (mm^{-1})	0.48	3.119
F(000)	1912	1992
Crystal size (mm^3)	$0.58 \times 0.36 \times 0.30$	$1.20 \times 0.60 \times 0.30$
Theta range for data collection (°)	1.45–26.40	1.45–29.89
Index ranges	$-13 \le h \le 13$, $-21 \le k \le 9$, $-27 \le l \le 27$	$-9 \le h \le 15$, $-23 \le k \le 22$, $-32 \le l \le 31$
Reflections collected	23816	32182
Independent reflections	8813 [$R_{int} = 0.0342$]	11382 [$R_{int} = 0.0411$]
Completeness	98.3% to theta = 26.40°	92.4% to theta = 29.89°
Refinement method	Full-matrix least-squares on F^2	Full-matrix least-squares on F^2
Data/restraints/parameters	8813/19/514	11382/0/533
Goodness-of-fit on F^2	1.041	1.072
Final R indices [$I > 2\sigma(I)$]	$R_1 = 0.0497$, $wR_2 = 0.1223$	$R_1 = 0.0310$, $wR_2 = 0.0737$
R indices (all data)	$R_1 = 0.0703$, $wR_2 = 0.1364$	$R_1 = 0.0358$, $wR_2 = 0.0765$
Absolute structure parameter	−0.05(3)	−0.014(5)
Largest difference peak and hole (e Å^{-3})	0.726 and −0.515	0.786 and −1.173

C*H*-*i*-Pr and *H*-4), 1.71 (m, *H*-4′, *H*-7, and *H*-7′), 1.13 (d, $^3J_{HH} = 6.8$, Me), 0.87 (d, $^3J_{HH} = 6.8$, Me). ^{13}C-NMR (CD_2Cl_2, 298 K, 400 MHz): 99.1 (q, $^1J_{RhC} = 8.1$, $^2J_{PC} = 12.4$, *C*-1), 97.6 (q, $^1J_{RhC} = 8.7$, $^2J_{PC} = 11.2$, *C*-2), 82.5 (d, $^1J_{RhC} = 12.4$, *C*-5), 77.4 (d, $^1J_{RhC} = 12.2$, *C*-6), 72.3 (s, *C*HN), 71.9 (s, *C*HO), 32.2 (s, *C*H-*i*-Pr), 30.6 (s, *C*-4), 30.5 (s, *C*-7), 29.5 (s, *C*-8), 29.3 (s, *C*-3), 20.9 (s, Me), 15.7 (s, Me). ^{31}P-NMR (CD_2Cl_2, 298 K, 400 MHz): 21.7 (d, $^1J_{RhP} = 147$ Hz).

*4.2.2. Complex **15b***

This was prepared in similar manner to **15a** using $[Ir(COD)_2]BF_4$ (25 mg, 0.05 mmol). Yield: 45 mg, 95%. MS (FAB): 845 (M^+–BF_4^-) (100). Single crystal suitable for X-ray diffraction was obtained from CH_2Cl_2–ether. Anal. Calc. for $C_{46}H_{44}NOBF_4PIr$ (936.86): C, 58.97; H, 4.73; N, 1.50. Found: C, 58.83; H, 4.85; N, 1.53. ^{1}H-NMR (CD_2Cl_2, 298 K, 400 MHz): 5.22 (br, *H*-1), 4.42 (br, *H*-2), 4.18 (t, $^2J_{HH} = 10.6$, $^3J_{HH} = 9.3$, *cis* C*H*O), 3.72 (t, $^2J_{HH} = 10.6$, $^3J_{HH} = 9.4$, *trans* C*H*O), 3.39 (m, C*H*N), 3.06 (br, *H*-6), 2.97 (br, *H*-5), 2.24 (m, *H*-8), 2.19 (m, C*H*-*i*-Pr), 2.05 (m, *H*-3), 1.95 (m, *H*-8′ and *H*-4), 1.77 (m, *H*-4′), 1.70 (m, *H*-7), 1.58 (m, *H*-3′), 1.38 (d, $^3J_{HH} = 6.7$, Me), 1.34 (m, *H*-7′), 0.92 (d, $^3J_{HH} = 6.7$, Me). ^{13}C-NMR (CD_2Cl_2, 298 K, 400 MHz): 89.7 (d, $^2J_{PC} = 10.7$, *C*-1), 82.4 (d, $^2J_{PC} = 15.0$, *C*-2), 74.9 (s, *C*HN), 72.8 (s, *C*-5), 72.6 (s, *C*HO), 62.4 (s, *C*-6), 34.4 (s, *C*-4), 32.6 (s, *C*-8), 30.6 (s, *C*H-*i*-Pr), 29.2 (s, *C*-7), 28.1 (s, *C*-3), 22.6 (s, Me), 16.7 (s, Me). ^{31}P-NMR (CD_2Cl_2, 298 K, 400 MHz): 18.5 (s).

*4.2.3. Complex **16***

A solution of $[Rh(COD)_2]BF_4$ (20 mg, 0.05 mmol) and ligand **11** (25 mg, 0.05 mmol) in CH_2Cl_2 (2 ml) was stirred at r.t. for 2 h. The solvent was evaporated i.v. and the residue was washed with hexane. Complex **16** was obtained as small needles from CH_2Cl_2–ether. Yield: 30 mg, 77%. MS (FAB): 707 (M^+–BF_4^-) (100). Anal. Calc. for $C_{38}H_{37}O_3BF_4PSRh$ (794.46): C, 57.45; H, 4.96. Found: C, 57.34; H, 4.91. ^{1}H-NMR (CD_2Cl_2, 298 K, 400 MHz): 5.92 (m, C*H*O), 5.95 (br, H-2), 5.74 (br, H-1), 5.10 (br, H-5), 3.67 (br, H-6), 3.48 (br d, $^2J_{HH} = 13.9$, *cis* SCH_2), 3.37 (m, CH_2–Et), 3.17 (m, CH_2–Et), 2.83 (q, $^2J_{HH} = 14.0$, $^3J_{HH} = 11.0$, *trans* SCH_2), 2.60 (m, H-3 and H-4), 2.49 (m, H-8 and H-8′), 2.45 (m, H-4′), 2.38 (m, H-3′), 2.20 (m, H-7′), 2.03 (m, H-7), 1.66 (t, $^3J_{HH} = 7.4$, $^3J_{HH} = 7.7$, Me). ^{13}C-NMR (CD_2Cl_2, 298 K, 400 MHz): 116.5 (q, ^1J(Rh,C), 5.0, ^2J(P,C), 12.9, C-2), 113.6 (q, ^1J(Rh,C), 5.7, ^2J(P,C), 12.9, *C*-1), 92.1 (d, ^1J(Rh,C), 10.1, *C*-5), 86.6 (d, ^1J(Rh,C), 9.2, *C*-6), 80.1 (s, *C*HO), 40.8 (s, S*C*H_2), 35.8 (s, *C*H_2–Et), 32.0 (s, *C*-8), 31.4 (s, *C*-7), 28.9 (s, *C*-4), 28.7 (s, *C*-3), 15.2 (s, Me) ^{31}P-NMR (CD_2Cl_2, 298 K, 400 MHz): 137.6 (d, $^1J_{RhP} = 195$). ^{103}Rh-NMR (CD_2Cl_2, 298 K, 400 MHz): -204 (d, $^1J_{RhP} = 190$).

*4.2.4. Complex **12***

This ferrocene complex was prepared in a similar manner to **16**. From 20 mg of the $[Rh(1,5\text{-}COD)_2]BF_4$ and 30 mg of **7** were obtained 38 mg (86%) of the product. Anal. Calc. for $C_{44}H_{56}BF_4P_2FeRh$ (892.43): C, 59.22; H, 6.32. Found: C, 59.05; H, 6.39. MS (FAB): 805 (M^+–BF_4^-) (62.4), 695 (100). ^{1}H-NMR (CD_2Cl_2, 298 K, 400 MHz): 5.56 (br, H-1), 5.36 (br, H-2), 4.32 (br, H-5), 3.86 (br, Cp), 3.32 (H-6), 2.43 (m, H-4 and H-4′), 2.34 (m, H-3′), 2.20 (m, H-3), 1.79 (m, H-8), 1.77 (m, H-7 and H-7′), 1.28 (m, H-8′). ^{13}C-NMR (CD_2Cl_2, 298 K, 400 MHz): 101.2 (s, C-6), 97.6 (s, C-1), 95.8 (s, C-5), 93.3 (s, C-2), 71.8 (s, Cp). ^{31}P-NMR (CD_2Cl_2, 298 K, 400 MHz): 53.5 (d, $^1J_{RhP} = 150$, *P*Cy$_2$), 21.4 (q, $^1J_{RhP} = 149$, $^2J_{PP} = 32$, *P*ph$_2$). ^{103}Rh-NMR (CD_2Cl_2, 298 K, 400 MHz): -229 (t, $^1J_{RhP} = 150$, $^1J_{RhP} = 148$).

*4.2.5. Complex **14***

This was kindly provided by Dr H. Rüegger [29]. ^{1}H-NMR (CD_2Cl_2, 298 K, 400 MHz): 4.47 (br, *H*-1 and *H*-2), 3.61 (br, *H*-5 and *H*-6), 2.48 (s, Me), 2.40 (m, *H*-8 and *H*-8′), 1.67 (m, *H*-4 and *H*-4′), 1.44 (m, *H*-3 and *H*-3′), 1.25 (m, *H*-7 and *H*-7′), 0.43 (s, B–Me). ^{13}C-NMR (CD_2Cl_2, 298 K, 400 MHz): 80.2 (8s, *C*-5 and *C*-6), 78.0 (s, *C*-1 and *C*-2), 30.4 (s, *C*-8), 30.3 (s, *C*-4), 29.0 (s, *C*-7), 28.8 (s, *C*-3), 15.1 (s, Me), 11.6 (s, B-Me). ^{103}Rh-NMR (CD_2Cl_2, 298 K, 400 MHz): 1134 (s).

5. Supplementary material

Two full numbering schemes for the diffraction results on **15a** and **15b** (2 pages), plus tables of atomic coordinates, bond lengths, bond angles, anisotropic displacement parameters and hydrogen coordinates for **15a** and **15b** (17 pages) are available on request from the author.

Acknowledgements

P.S.P. thanks the Swiss National Science Foundation and the ETH Zurich for financial support. We also thank F. Hoffmann–La Roche AG, Basel, for the MeO–Biphep ligand, Professor A. Togni for ferrocene ligand **7** as well as Johnson Matthey for the loan of $RhCl_3$. Special thanks are due Dr Heinz Rüegger for the loan of complex **14** and for helpful discussions.

References

[1] (a) J.M. Brown, Chem. Soc. Rev. (1993) 25. (b) J.A. Ramsden, T.D.W. Claridge, J.M. Brown, J. Chem. Soc. Chem. Commun.

(1995) 2469. (c) E. Fernandez, M.W. Hooper, F.I. Knight, J.M. Brown, J. Chem. Soc. Chem. Commun. (1997) 173 and Refs. therein.
[2] Z. Zhou, B.R. James, H. Alper, Organometallics 14 (1995) 4209.
[3] A. Togni, C. Breutel, A. Schnyder, F. Spindler, H. Landert, A. Tijani, J. Am. Chem. Soc. 116 (1994) 4062.
[4] H. Kumobayashi, Rec. Trav. Chim. Pays-Bas 115 (1996) 201.
[5] A. Roucoux, L. Thieffry, J. Carpentier, M. Devocelle, C. Meliet, F. Agboussou, A. Mortreux, A.J. Welch, Organometallics 15 (1996) 2440.
[6] M.J. Burk, J.E. Feaster, R.L. Harlow, Tetrahedron: Asymmetry 2 (1991) 569.
[7] B.E. Mann, B.F. Taylor, ^{13}C NMR Data for Organometallic Compounds, Academic Press, London, 1981.
[8] M.J. Burk, J.E. Feaster, W.A. Nugent, R.L. Harlow, J. Am. Chem. Soc. 115 (1993) 10125.
[9] A. Marinetti, C. Le Menn, L. Ricard, Organometallics 14 (1995) 4983.
[10] X. Zhang, K. Mashima, K. Koyano, N. Sayo, H. Kumobayashi, S. Akutagawa, H. Takaya, J. Chem. Soc. Perkin Trans. (1994) 2309.
[11] E. Cesarotti, A. Chiesa, G. Ciani, A. Sironi, J. Organomet. Chem. 251 (1983) 79.
[12] J. Bakos, I. Toth, B. Heil, G. Szalontai, L. Parkanyi, V. Fulop, J. Organomet. Chem. 370 (1989) 263.
[13] A.G. Avent, R.B. Bedford, P.A. Chaloner, S.Z. Dewa, P.B. Hitchcock, J. Chem. Soc. Dalton Trans. (1996) 4633.
[14] T. Yoshida, K. Tani, T. Yamagata, Y. Tatsuno, T. Saito, J. Chem. Soc. Chem. Commun. (1990) 292.
[15] H. Yang, N. Lugan, R. Mathieu, Organometallics 16 (1997) 2089.
[16] N. Feiken, P.S. Pregosin, G. Trabesinger, Organometallics 17 (1998) 4510.
[17] A. Albinati, J. Eckert, P.S. Pregosin, H. Rüegger, R. Salzmann, C. Stössel, Organometallics 16 (1997) 579.
[18] H. Berger, R. Nesper, P.S. Pregosin, H. Rüegger, M. Wörle, Helv. Chim. Acta 76 (1993) 1520.
[19] (a) J.M. Brown, J.J. Perez-Torrente, Organometallics 14 (1995) 1195. (b) M.T. Ashby, M.A. Khan, J. Halpern, Organometallics 10 (1991) 2011.
[20] (a) K. Mashima, K. Kusano, T. Ohta, R. Noyori, H. Takaya, J. Chem. Soc. Chem. Commun. (1989) 466. (b) T. Ohta, H. Takaya, R. Noyori, Inorg. Chem. 27 (1988) 566. (c) K. Toriumi, T. Ito, H. Takaya, T. Souchi, R. Noyori, Acta Crystallogr. Sect. B 38 (1982) 807.
[21] K. Selvakumar, M. Valentini, M. Wörle, P.S. Pregosin, A. Albinati, Organometallics 18 (1999) 1207.
[22] P.S. Pregosin, R. Salzmann, Coord. Chem. Rev. 155 (1996) 35.
[23] P.S. Pregosin, G. Trabesinger, J. Chem. Soc. Dalton Trans. (1998) 727.
[24] (a) B.R. Bender, M. Koller, D. Nanz, W. von Philipsborn, J. Am. Chem. Soc. 115 (1993) 5889 and M.G. Partridge, B.A. Messerle, L.D. Field, Organometallics 14 (1995) 3527 represent nice examples of exchange spectroscopy related to Rh–phosphine catalysts.
[25] A. Gogoll, J. Ornebro, H. Grennberg, J.E. Bäckvall, J. Am. Chem. Soc. 116 (1994) 3631.
[26] T.G. Schenck, J.M. Downes, C.R.C. Milne, P.B. Mackenzie, H. Boucher, J. Whelan, B. Bosnich, Inorg. Chem. 24 (1985) 2334.
[27] SADABS, G. Sheldrick, Göttingen, Germany, 1997.
[28] SHELXTL program package, Version 5.1, Bruker AXS, Inc., Madison, WI, USA.
[29] M. Bortolin, U.E. Bucher, H. Rüegger, L.M. Venanzi, A. Albinati, F. Lianza, S. Trofimenko, Organometallics 11 (1992) 2514.